Heliyon 10 (2024) e30649

Contents lists available at ScienceDirect

Heliyon

journal homepage: www.cell.com/heliyon

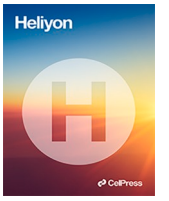

Research article

A novel microfluidic chip integrated with Pt micro-thermometer for temperature measurement at the single-cell level

Kai Chen [a,d,1], Baihui Liang [b,c,1], Ping Yang [a], Min Li [a], Haojun Yuan [a], Jinlei Wu [a], Wanlei Gao [a,d,*], Qinghui Jin [a,d]

[a] College of Information Science and Engineering, Ningbo University, Ningbo, 315211, Zhejiang, China
[b] Healthy & Intelligent Kitchen Engineering Research Center of Zhejiang Province, Ningbo, 315336, Zhejiang, China
[c] Ningbo Fotile Kitchen Ware Company, Ningbo, 315336, Zhejiang, China
[d] State Key Laboratory of Transducer Technology, Shanghai Institute of Microsystem and Information Technology, Chinese Academy of Sciences, Shanghai, 200050, China

ARTICLE INFO

Keywords:
Single cell isolation
Pt electrode-based thermometer
Microfluidic chip
In-situ temperature detection
Tumor cell analysis

ABSTRACT

Noninvasive and sensitive thermometry of a single cell during the normal physiological process is crucial for analyzing fundamental cellular metabolism and applications to cancer treatment. However, current thermometers generally sense the average temperature variation for many cells, thereby failing to obtain real-time and continuous data of an individual cell. In this study, we employed platinum (Pt) electrodes to construct an integrated microfluidic chip as a single-cell thermometer. The single-cell isolation unit in the microchip consisted of a main channel, which was connected to the inlet and outlet of a single-cell capture funnel. A single cell can be trapped in the funnel and the remaining cells can bypass and flow along the main channel to the outlet. The best capture ratio of a single MCF7 cell at a single-cell isolation unit was 90 % under optimal condition. The thermometer in the micro-chip had a temperature resolution of 0.007 °C and showed a good linear relationship in the range of 20–40 °C ($R^2 = 0.9999$). Slight temperature increment of different single tumor cell (MCF7 cell, H1975 cell, and HepG2 cell) cultured on the chip was continuously recorded under normal physiological condition. In addition, the temperature variation of single MCF7 cell in-situ after exposure to a stimulus (4 % paraformaldehyde treatment) was also monitored, showing an amplitude of temperature fluctuations gradually decreased over time. Taken together, this integrated microchip is a practical tool for detecting the change in the temperature of a single cell in real-time, thereby offering valuable information for the drug screening, diagnosis, and treatment of cancer.

1. Introduction

Temperature is a crucial parameter in many physiological indices [1]. It is involved in the biochemical reactions of many cells and is a critical parameter index for maintaining the function of organisms [2]. Therefore, detecting the temperature of all cells can provide substantial information for studying cell behavior and interactions [3]. While the behaviors of a single cell make difference to many life

* Corresponding author. The Faculty of Electrical Engineering and Computer Science, Ningbo University, Ningbo, Zhejiang, 315211, China.
E-mail address: gaowanlei@nbu.edu.cn (W. Gao).
[1] These authors contributed equally.

https://doi.org/10.1016/j.heliyon.2024.e30649
Received 9 November 2023; Received in revised form 27 March 2024; Accepted 1 May 2024
Available online 4 May 2024

processes, especially tumorigenesis. Tumor cell heterogeneity refers to genotype to phenotype differences in individual tumor cells in different parts of the same malignant tumor or different parts of the same patient [4]. Compared to the overall analysis of cell populations, temperature can be detected at the single-cell level, and thus represents a novel tool for analyzing cellular status from a new aspect, which will offer new insights into cell biology [5,6].

Current methods for single-cell temperature measurement can be categorized as contactless measurement and contact measurement. Some contactless intracellular thermometry methods make use of temperature-sensitive materials, including quantum dot, nanogels, and fluorescent dyes [3,7–9]. The temperature of a single cell is usually presented by the fluorescence intensity or spectra of these materials. The accuracy of many luminescence thermometers is disturbed by many other environmental factors, such as pH, ion concentration, and pressure. Recently some researchers have developed some new polymeric nano-thermometers for measuring cellular temperature, which can partially overcome the issue of their cross-sensitivity to environmental factors [10,11]. Although the new temperature-sensitive materials are less affected by the environment, their introduction into cells for detecting temperature changes through imaging methods may partially impact the normal metabolic activities of the cells. Moreover, the accuracy of temperature detection in these methods relies entirely on the performance of large-scale imaging instruments. Therefore, these luminescence thermometers are unsuitable for real-time and long-term monitoring of live single cells in situ. In addition, some micro-probes can be used to detect the temperature of single cells in contact. The spider silk fiber probe decorated with an up-conversion nanoparticle was used for detecting the membrane temperature of a single breast cancer cell, achieving a sensitivity of 0.0033–0.0045 °C [12]. A nanopipette-based thermocouple probe, in which carbon and platinum (Pt) were used as inner and outer electrodes, respectively, was developed for single-cell temperature sensing. The temperature resolution of this thermocouple probe was 0.08–0.24 °C [13]. However, as the microprobe must be positioned on a single cell, detecting temperature based on probes required an expensive micromanipulation instrument and professional operation.

Thin-film electrode-based electric thermometers provide another choice for invasively and simply sensing cell temperature. In general, measuring systems used for electric thermometers are considerably cheaper than those used for luminescence thermometers [14,15]. A micro-thin-film thermocouple array was prepared with Pd and Cr thin-film electrodes for monitoring the temperature increment of live cells [16]. In addition, a Pt thin-film-based temperature sensor was integrated into a biosensor to monitor temperature variations in HeLa cancer cells [2]. However, both the Pd and Cr thin-film thermocouple array and Pt thin-film thermometer were integrated into an open and large chamber for culturing cells and detecting their temperature [17,18]. These sensors cannot capture single cells and monitor the temperature at the single-cell level.

Recently, microfluidic chips have rapidly developed into a relatively independent and highly interdisciplinary field, thereby occupying a leading position in analytical chemistry, life science, and other fields [19,20]. Microfluidic technology can effectively integrate single-cell capture and high-sensitivity real-time dynamic analysis on a single chip [21]. We developed a Pt thermo-sensor-based microfluidic chip, integrating the functions of cell trapping and culturing, and temperature detection. Temperature fluctuation in a few tumor cells (as low as 7 cells) cultured on a chip can be monitored with this chip under normal physiological conditions [22].

To detect and monitor temperature fluctuation at a single-cell level, we utilized the Pt microelectrode-integrated microchip in this study. A funnel-shaped well was designed in the microchip to isolate a single cell from the cell suspension and then to culture it in situ. A snake-shaped thin-film Pt electrode was applied under the bottom of the single-cell isolation well to sense temperature change in the captured cell. The accuracy, sensitivity, and reproducibility of the microfluidic chip were tested to validate the performance of the temperature sensor. Different single tumor cell (MCF7 cell, H1975 cell, and HepG2 cell) was captured and cultured on this microchip, respectively. The Pt-based microsensor recorded the temperature variation of the trapped cell under the normal state or after exposure to a stimulus (4 % paraformaldehyde treatment). The microfluidic chip combined with the thin-film Pt electrode can offer a promising platform for real-time monitoring of the temperature variation of a single cell, thereby promoting the development of drug screening, disease diagnosis, and treatment [23,24].

2. Materials and methods

2.1. Chip fabrication

The chip is mainly composed of two parts: a microchannel layer and a glass electrode layer. The microchannel layer contains a specific structure that allows the capture of single cells. The glass electrode layer is composed of a glass substrate and a temperature measurement electrode for high-precision monitoring of temperature fluctuations in a single cell. Photolithography technology was used for fabricating the mold of the microchannel layer. First, the silicon wafer was cleaned using a plasma cleaning machine. Then, microchannels of 20-μm height were formed through photolithography and deep reactive ion etching. After the etching was completed, the silicon wafer was ultrasonically cleaned with acetone and isopropanol, dried, and a mold was formed. A polydimethylsiloxane (PDMS) mixture of the base and curing agent (w:w = 10:1) (Sylgard 184, Dow Corning, Midland, Michigan, USA) was processed in a vacuum oven to remove bubbles. Subsequently, the processed mixture was poured on the Si mold and incubated at 90 °C for 1 h in an oven. Lastly, the cured PDMS was peeled off the mold and cut into single PDMS chips.

The glass electrode layer was fabricated through a standard microelectromechanical process (Fig. S1). First, a 50-nm-thick Cr layer was sputtered on a 4 inch glass sheet (BF33, Schott Glaswerke AG) as the adhesion layer, and then, a 50-nm-thick Pt layer was sputtered as the electrode of temperature detection with magnetron sputtering instrument(Explorer14, Denton, USA). Then, microstructures were formed using LC100A photoresist with a photolithography machine (MA6, Germany SUSS Micro Tec). The wafer was etched through ion beam processing (Ion fab 300 plus, Oxford instruments, England) for removing Cr and Pt layers. After removing

the photoresist, the chip was covered with a 500-nm-thick Si_3N_4 layer as an insulating material through plasma-enhanced chemical vapor deposition (plasmalab system 100, Oxford instruments, England). Finally, the Si_3N_4 layer on the part of the solder joint was removed through photolithography and reactive ion etching(RIE-101iPH, Samco, Japan). The single electrode chip was formed by dicing. The electrode and PDMS chips were bonded as the alignment mark through plasma treatment by a plasma cleaner(TS-PLSY05, TONSON TECH, Shenzhen, China). The aligned chip was then incubated at 120 °C for 1 h to strengthen the bonding of the two parts of the chip.

2.2. Cell culture and sampling

Breast cancer cells (MCF7), hepatoma carcinoma cell (HepG2), and lung adenocarcinoma cell (H1975 cell) were purchased from the Chinese Academy of Sciences cell bank. MCF7 cells were cultured in minimum essential medium (MEM) (Gibco) with 10 % fetal bovine serum (FBS), 1 % MEM non-essential amino acids solution (Gibco), 1 % sodium pyruvate, 1 % glutamax, 1 % penicillin mixture, and 0.01 mg/mL human recombinant insulin. H1975 cells were cultured in Roswell Park Memorial Institute (RPMI)1640 medium (Gibco) supplemented with 10 % FBS. The HepG2 cell lines were cultured in Dulbecco's Modified Eagle Medium (DMEM, Gibco) supplemented with 10 % FBS.

The MCF7, HepG2 and H1975 cells were cultured in the medium for 1 week and collected in the medium after trypsin treatment. The concentration of cells in the collected sample was measured using a hemocytometer. Before capturing a single cell, the microchips were sterilized in high-pressure steam boilers for 20 min and dried at 80 °C for 4 h. Subsequently, the culture medium for the cells was introduced into the microchip through a peristaltic pump (L100-1S-2, Longer Precision Pump Co., Ltd.). The cell suspension was injected into the microchip through the peristaltic pump. If a single cell was observed in the chip under the microscope, the chip was transferred to the cell incubator for culturing that cell. To prevent evaporation of the medium, the inlet and outlet of the microchip were sealed with pipette tips, which were filled with the cell culture medium.

2.3. Identification of cell viability

To identify cell activity, a mixture of 5 μM calcein-AM and 0.5 μM propidium iodide (PI) was injected into the microchip containing the trapped cells. Then, the chip was incubated at room temperature. After 30 min, PBS was introduced into the chip for dye solution removal. Lastly, cell viability was identified under the fluorescence channel (Ex: 480 nm, Em: 515 nm) of a fluorescence microscope (WMF-XD, Shanghai WUMO, China). Cells with green fluorescence were considered live cells. Cells that emitted only red fluorescence were considered dead.

2.4. Sensor calibration

Before detection, the thermal sensor in the microfluidic chip was calibrated in a high-precision constant temperature water tank (SCIENTZ, GH-30A). By using an electrochemical workstation (GAMRY reference 600+), the resistance of the Pt sensor unit was detected between 30 °C and 40 °C in the constant current scanning mode. The temperature value (T) and the corresponding resistance value (R) were fitted as follows: $R = aT + b$, where a was the linear coefficient and b was the intercept.

2.5. Measurement of temperature fluctuation in a single cell

The chip contains two electrode pairs. One electrode is covered with a single-cell capture structure and is called the working electrode, and the other electrode is in the microchannel without a single-cell capture structure and is called the control electrode. First, the chip was placed in the high-precision constant temperature water tank, and the resistance of the two electrode pairs was measured at the same time. The temperature fluctuation value of the live cell was calculated as follows:

$$\Delta T_{cell} = T_{WE} - T_{CON}$$

Where, ΔT_{cell}, T_{WE}, T_{CON} denoted the fluctuation value of the cell temperature, temperature of the area with a cell, and the environmental temperature outside the cell.

2.6. Statistical analysis

Data obtained from the electrochemical workstation were imported into Origin 8.5 for performing statistical analysis, and temperature values were calculated according to the linearity curve.

3. Results and discussion

3.1. Design and characterization of the Pt thermometer-integrated microfluidic chip

We developed a microfluidic chip for temperature detection at a single-cell level. It included a microchannel layer for the isolation and culture of a single cell, and a thin-film Pt electrode chip that acted as the thermometer (Fig. 2a). Based on a capture pocket for

single cell isolation in the previous study, a microfluidic chip for capturing single cell was developed with some modification [25]. The structure in the microchip for single-cell isolation consisted of a 100-μm-diameter cell capture funnel well, whose top part and the drain channel were connected two parts of the same main channel, respectively (Fig. 1a and b). The main channel was 50-μm wide and 20-μm deep to ensure the cells flow as a monolayer. When the cell suspension was injected into main channel, the cell capture funnel well could capture the cell gently. A single cell would be trapped at the bottom of the semicylindrical funnel (facing the entrance of the drain channel) and settle within the funnel. This was because the flow into the drain channel, which initially guided the cell into the chamber, was partially jammed and slowed down by the captured cell. According to the design of the microchannels, when the cell capture funnel was empty, the flow resistance in the drain channel was minimal and the cell passing through the cell capture funnel was captured. Once the cell was trapped in the funnel, the flow resistance in the drain channel became maximal so that the other cells could pass over or through and out of the cell capture funnel.

To investigate the validity of the single-cell isolation funnel, the microfluidic chip was numerically simulated using COMSOL Multiphysics software. A 2D laminar flow model based on the steady-state Navier–Stokes'equation was used for the simulation. Water, with a density of 1000 kg/m^3 and a dynamic viscosity of 0.001 Pa·s, was selected as the fluid, and an incompressible flow model was applied. The boundary conditions of 400 μm/s and zero pressure were used at the inlet and outlet, respectively, and no-slip conditions were applied to all walls. The flow rate profile is presented in Fig. 1c. The width of the drain channel can affect the effect of single-cell isolation. Simulation model 1 with a 5-μm-wide drain channel, and simulation model 2 with a 10-μm-wide drain channel were established. Four velocity probes were selected from different locations of the flow field. Probes A and B were located at the inlets of the

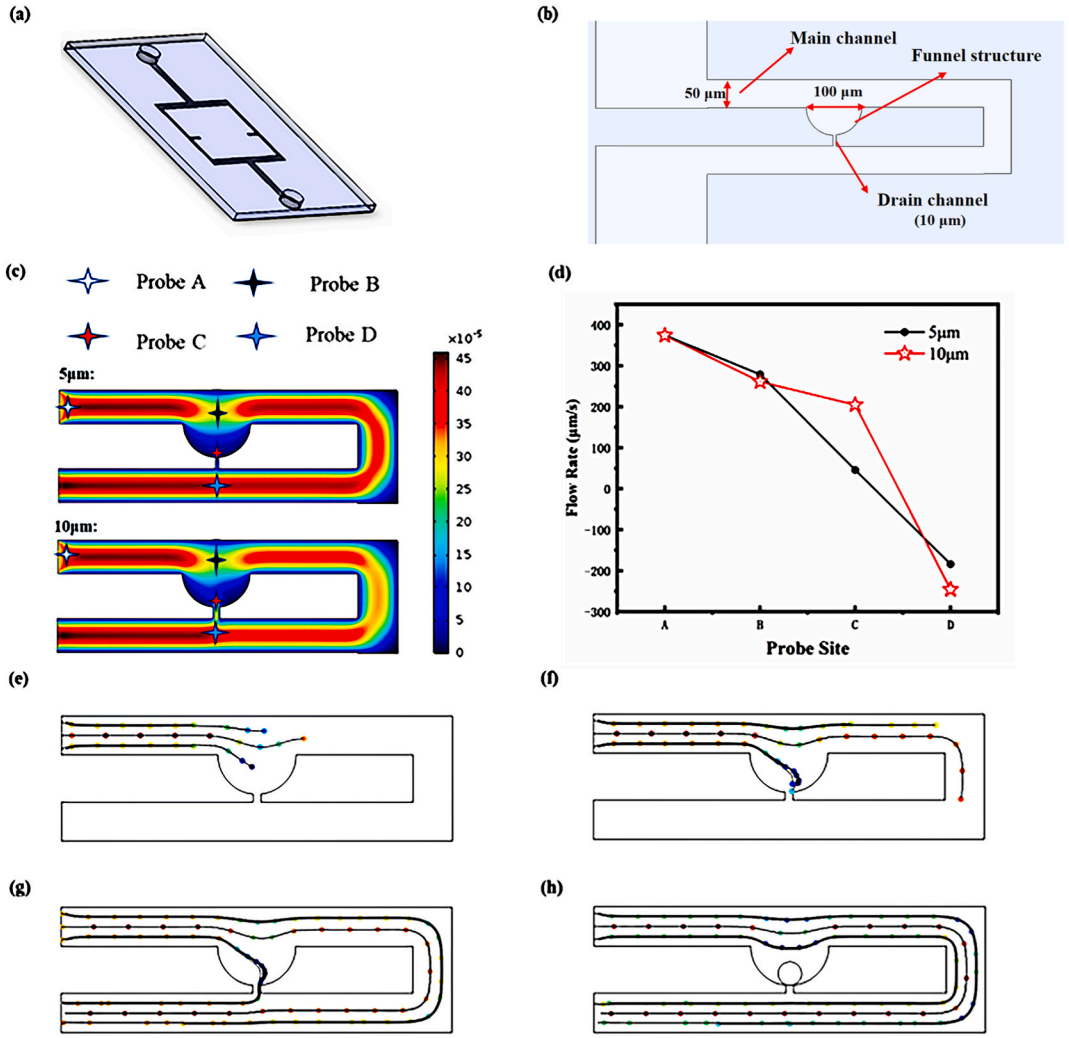

Fig. 1. Flow field analysis of COMSOL Multiphysics. (a) The diagram of the microfluidic chip. (b) The specific dimensions of the isolation unit. (c) Velocity profiles for the isolation unit with a 5-μm drain channel (Model 1) and the isolation unit with a 10-μm drain channel (Model 2). The four crosses in the flow field represent four velocity probes, which were labeled as A, B, C, and D. (d) The flow rates of different probes in the two models. (e)–(g) The particle-tracing distribution around the isolation unit over time. (h) The particle-tracing distribution around the isolation unit when the drain channel is occupied.

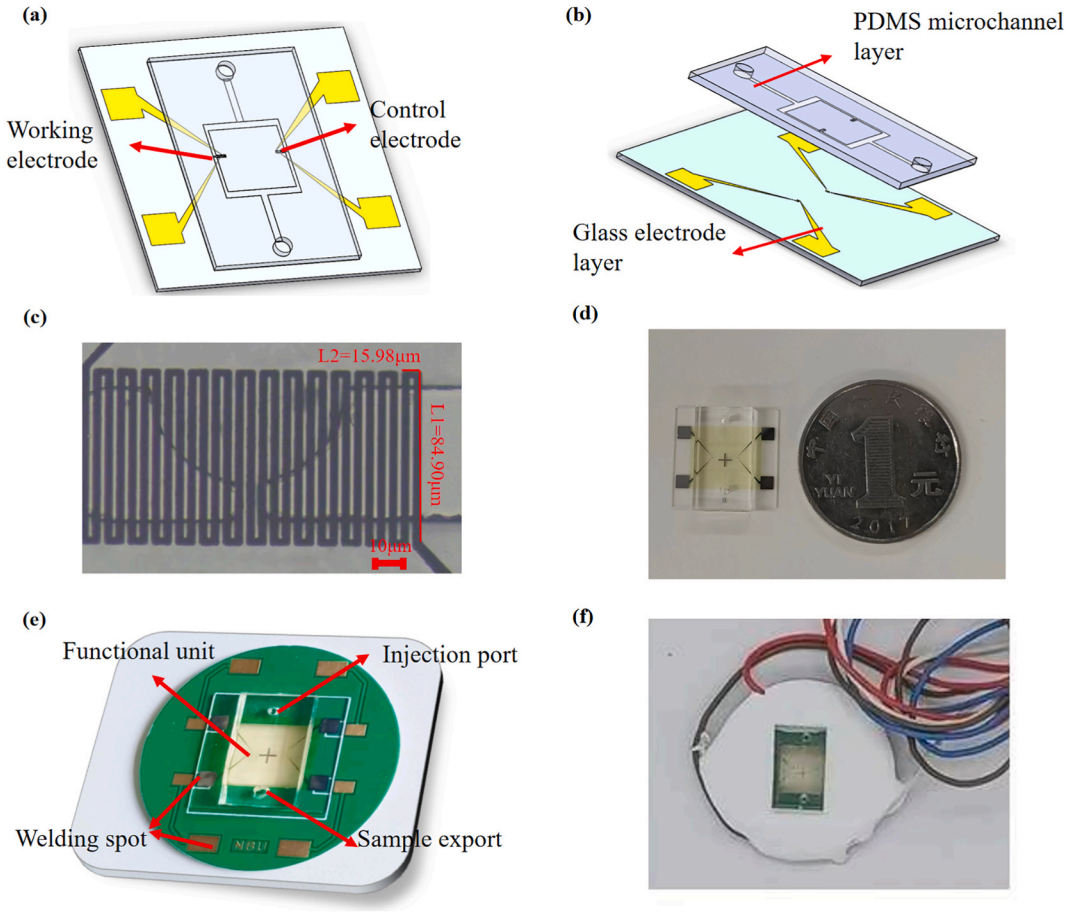

Fig. 2. System diagram of Pt thermometer-integrated microfluidic chip. (a) Schematic representation of the integrated device. (b) Schematic representation of the layered chip structure. (c) The top view of the single cell isolation unit and Pt electrodes. (d) An image of the whole micro-chip of size 15.8 mm × 15.0 mm. (e) A diagram of the micro-chip mounted with a PCB board. (f) An image of the micro-chip mounted with the PCB board.

main channel and funnel well, respectively. Probes C and D were placed at the inlet and outlet of the drain channel, respectively. Four flow rates in two models were compared, which were shown in Fig. 1d. The large flow rate meant a small flow resistance. The flow rate difference between Probes B and D produced a gentle flow in the drain channel, which provided the impetus required for the cell to enter the funnel well. The difference of the flow rate between Probes B and D for Model 2 was 506 μm/s, which was larger than that for Model 1 (462 μm/s). Therefore, the single cell preferred to flow into the funnel structure with a 10-μm-wide drain channel. Moreover, the trajectory of the cell in the microchannels for Model 1 and Model 2 was simulated after sampling. As depicted in Fig. 1d, in the funnel structure with a 10-μm-wide drain channel, the flow rate at Probe Site C was comparable to that at Probe Site B, indicating that the flow resistance at the main channel and capture funnel structure was similar for the cell. Therefore, the cell flowed into the capture funnel structure or along the main channel after entering the main-channel in Model 2 (Fig. 1e–f). When the drain channel was occupied, the cell bypassed the funnel structure and only flowed along the main channel (Fig. 1h). The inlet flow rate of the 5-μm-wide drain channel (Probe Site C) in Model 1 was significantly lower compared to that of Probe Site B, indicating a high flow resistance for cells to enter the funnel structure (Fig. 1d). Cells only preferred to flow along the main channel whether the funnel structure in the Model 1 was occupied or not (Fig. S2). Therefore, the isolation funnel structure with a 10-μm-wide drain channel was suitable for single-cell capture.

The thin-film Pt electrode layer is aligned to the microfluidic layer (Fig. 2a). Two parallel main channels are present in the microfluidic chip: one connected to the single-cell isolation funnel and the other serving as a blank control. Therefore, a Pt electrode pair is located in the main channels (Fig. 2b), with one under the bottom of the single-cell isolation funnel called the working electrode and the other control electrode at the other main channel without a single-cell isolation funnel for sensing the temperature variation of the environment. The thin-film Pt electrode was formed by sputtering the electrode pattern on the glass substrate. As shown in Fig. 2c, temperature sensor is composed of 29 gate-type platinum electrodes, each with a length of 84.9 μm, and width and spacing of 5 μm. As a single cell enters the capture funnel structure through the microstructure, the heat generated by the cell is transferred to the Pt wire electrode, causing the resistance value of the electrode to change. To measure the temperature of the cell, the constant current method

was used to determine the linear relationship between resistance and temperature. For detection, the ends of the Pt thin-film-based resistor were connected to an external device (Gamry reference600) having a high voltage resolution. To reduce the thermal effect of thermal resistance, the current for temperature measurement was set to 30 μA. Because of the linear relationship between resistance and temperature transformations, the Pt thermal resistance wire exhibits the following relationship:

$$R = KT + b$$

Where, R is the Pt thermal resistance value, T is the temperature, K is the linear coefficient, and b is the intercept value.

After bonding the microfluidic layer and the Pt thermometer layer, the whole chip of length 15.8 mm and width 15 mm was fabricated (Fig. 2d). To facilitate testing, the chip had to be packaged on the printed circuit board (PCB) and sealed with a silicon sealant to form a separate chip device (Fig. 2e). As shown in Fig. 2f, the chip was welded on the PCB board through patch wiring and packaged with a sealant to form a complete measurement minimum unit.

3.2. Chip characterization and optimization using cell lines

The flow rate in the main channel was a crucial factor determining the effect of cell capture. The capture of individual single MCF7 cells was tested in the presence of the microfluidic chip with a glass substrate. A 10 μL suspension of MCF7 cells were injected into the microchip at various flow rates. Tests were performed using flow rates of 5, 10, and 20 mL/min, with 10 different chips employed for each flow rate condition. At 5 mL/min and 10 mL/min, single cells were successfully trapped in all chips, resulting in a capture rate of 100 %. As shown in Figs. S3a and 3b, under the flow rate of 10 mL/min, a small part of the cell was pushed into the narrow drain channel, which could stay more stable at the funnel structure. However, when the flow rate was set to 20 mL/min, no cells were observed in 7 chips, and distorted cells were found in 3 chips. To maintain the cell's integrity during isolation, the best flow rate for sampling was set to 10 mL/min.

The cell concentration in the sample was critical for high-efficiency single-cell capture. Excessive cells in the suspension for sampling will block channels. However, if the cell concentration is too low, the probability of single-cell isolation will decrease. To investigate the effect of cell suspension concentration on single-cell capture by the chip, 10 μL of the MCF7 cell suspension at different concentrations, namely 3.2×10^5/mL, 1.45×10^5/mL, and 4×10^4/mL, were injected into the microchip, respectively. Each test for one sample was conducted in 10 chips. The capture efficiency was defined as the ratio of the chip capturing a single cell. When the cell concentration was greater than 3.2×10^5/mL, 70 % chips were crowded with numerous cells (Fig. 3a and d). Because the sample contained many cell clusters, the clusters capped the narrow drain channel of the funnel and other single cells bypassed the funnel. When the concentration was decreased to 1.45×10^5/mL, 90 % chips trapped single cells (Fig. 3b and d). The capture efficiency for the lower cell concentration (4×10^4/mL) was only 60 %, while some chips failed to trap a cell (Fig. 3c and d). Therefore, if the sample concentration was approximately 1.45×10^5/mL, with no cell clusters, most cells trapped in the chip were single.

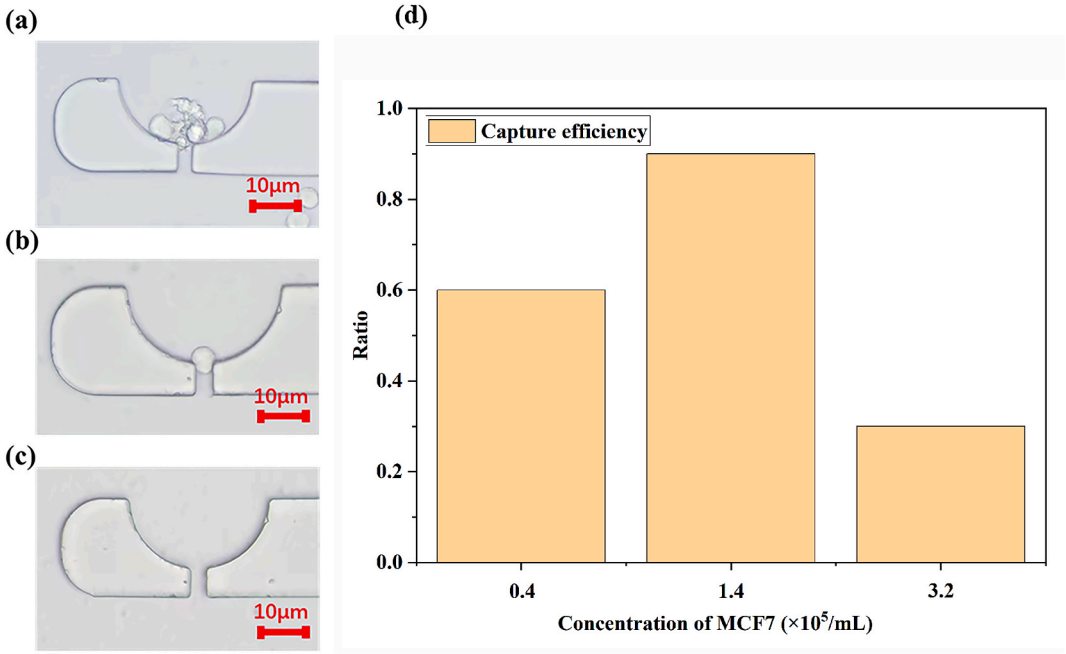

Fig. 3. Effect of cells' concentration on the capture efficiency for single-cell isolation. The morphology of cells in the isolation unit after sampling the cells' suspension at a concentration of 3.2×10^5/mL (a), 1.45×10^5/mL (b), and 4×10^4/mL (c). The capture efficiency of single cell for different samples with different cells' concentration (d).

3.3. Performance test of temperature sensor

The temperature variation of a single cell can only be detected if the Pt thermometer in the microchip met the characteristics of high resolution, high sensitivity, good repeatability, and low return error. To investigate the performance of the microsensor in the integrated chip, we conducted tests in the high-precision constant temperature water tank at a stability of 0.015 °C. After the water tank was stabilized, the Pt thermal sensor was placed in the tank for testing. Fig. 4 plots the calibration results of the Pt electrode sensor in the integrated chip. By setting sampling points at 2 °C intervals in the range of 30–40 °C, measurements of each temperature for the same chip were performed on days 1, 10, and 20, and the linear fitting curve of the temperature and the corresponding resistance was plotted. As shown in Fig. 4a, resistance (R) of the sensor had a stable and good linear relationship with temperature (T) over the long term ($R^2 = 0.9999$). A change of 1 °C resulted in a resistance change of 4.4737 Ω. Thus, the sensitivity of the sensor was 0.2235 °C/Ω. Based on the voltage resolution of the electrochemical workstation, which was 1 μV, the temperature resolution of the sensor was 0.007 °C.

To test the characteristic of hysteresis, the integrated chip was placed in the constant temperature water tank set between 30 °C and 40 °C. The resistance of the Pt sensor in the chip was recorded at each drop and rise in the temperature. As shown in Fig. 4b, the maximum return error occurred at 30 °C. At 30 °C, the maximum deviation value was 0.54 Ω and the hysteresis coefficient was 0.021 % (the maximum deviation/the resistance value at the highest temperature). At the optimum temperature for cell cultivation (37 °C), the temperature deviation of the tested chip was 0.024 °C (Fig. S4), which was considerably less than the average temperature difference of a single MCF7 cell during normal metabolism (0.37 ± 0.13 °C) [12]. Therefore, the microfluidic chip temperature sensor has the characteristics of good linearity, high sensitivity, and high temperature resolution and thus meets the requirement for temperature measurement at a single-cell level.

3.4. Temperature fluctuation of single living cell on chip

Our proposed microchip allowed trapping of a single cell by a chip, temperature detection, and monitoring of temperature fluctuation in a single cell in situ. High-precision temperature monitoring at a single-cell level can help understand single cell metabolism, thereby promoting research in the field of cell heterogeneity, especially that of tumor cells [26].

To evaluate the feasibility of in-situ monitoring of a single cell, a single MCF7 cell was isolated using the microchip, and the microchip was filled with the culture. The image of the isolation structure in the chip was presented in Fig. 5a. After sampling the culture, the trapped cell was allowed to stay in the funnel area without any deformation (Fig. 5b). Subsequently, the single cell on the chip was cultured for 24 h. To monitor the temperature variation of the single cell, the chip was placed in a water tank, which could maintain a constant temperature with a maximum fluctuation of 0.015 °C. The signal of the Pt sensor in the chip was received by a home-made PCB. After testing for 3 h in water, the vitality of the cell was determined using the mix dye (including 5 μM calcein-AM and 0.5 μM PI). As shown in Fig. 5c, the cell labeled green in the chip was alive, and this presented the feasibility of this microchip for long-term monitoring of a single cell's state.

To test temperature fluctuation in a single cell on the chip, the measurement of different tumor cell (MCF7 cell, H1975 cell, and HepG2 cell) on the chip was performed, respectively. The temperature change for alive MCF7 cell adherent to the sensor's surface was presented in Fig. 5d. Following a reduction of the background noise detected by the blank control unit, the maximum temperature fluctuation in the MCF7 single cell during the test was 0.721 °C and the minimum temperature fluctuation was −0.676 °C. The average change of temperature was 0.118 °C. Among the process of detection, the temperature of cell exceeded that of the environment for 394 s, accounting for 65.7 % of the entire process. The temperature variation of hepatoma carcinoma cell (HepG2) ranged from −0.093 °C

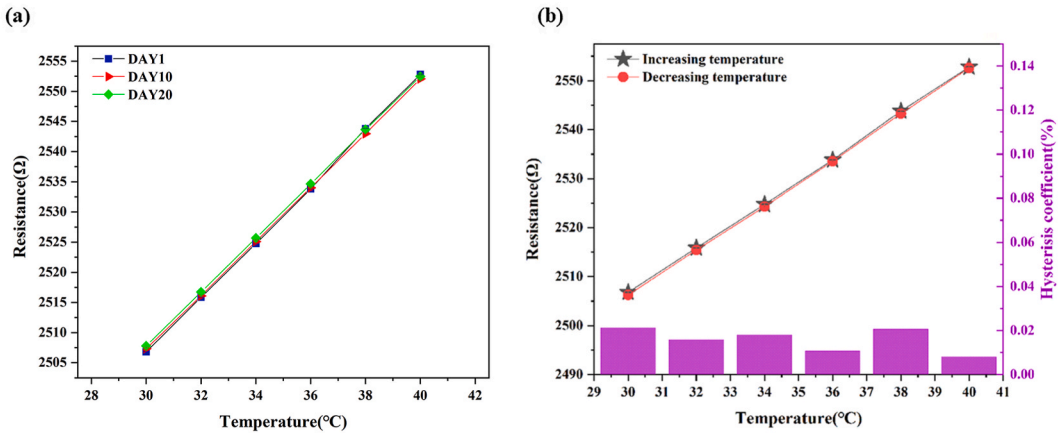

Fig. 4. The result of temperature sensor performance test. (a) When the temperature was 30–40 °C, the repeatability test of the temperature sensor was conducted on days 1, 10, and 20. (b) In the return error test of the temperature sensor, the maximum return error occurred at 30 °C, with the maximum deviation of 0.54 Ω and a relative variation of 0.01 %.

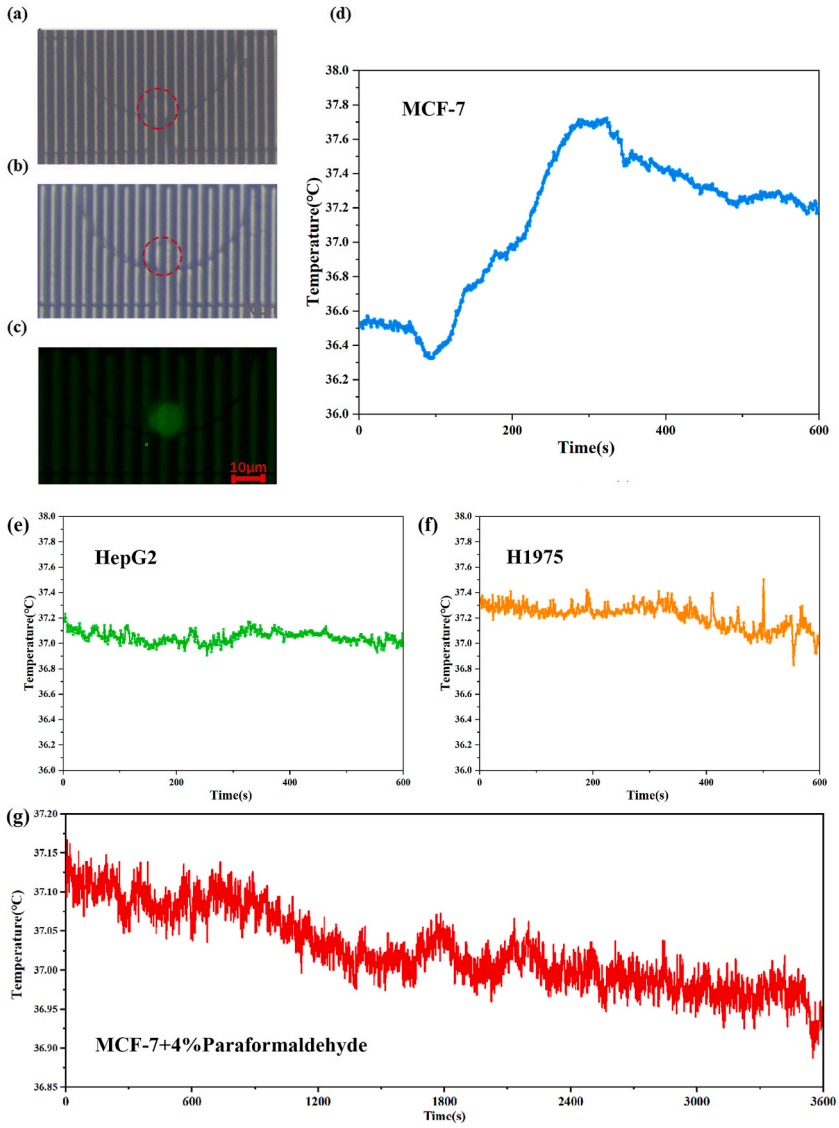

Fig. 5. The morphology of a single cell on chip and the cellular temperature fluctuation during the measurement. The morphology of a MCF7 cell in the isolation unit on chip before temperature measurement (a), after temperature measurement (b), and after calcein-AM/PI staining (c). The red cycle outlined contour of the cell. Temperature fluctuation of a single breast cancer cell (MCF7) (d), a single hepatoma carcinoma cell (HepG2) (e), and a single lung adenocarcinoma cell (H1975 cell) (f) during normal metabolism in a constant temperature water tank of 37 °C. (g) Temperature fluctuation of a single MCF7 cell during the treatment of 4 % paraformaldehyde in a constant temperature water tank of 37 °C. (For interpretation of the references to colour in this figure legend, the reader is referred to the Web version of this article.)

to 0.232 °C, which was smaller in comparison to the temperature variation observed in breast cancer cell (MCF7) (Fig. 5e). The temperature change of lung adenocarcinoma cell (H1975 cell) was between −0.171 °C and 0.502 °C with an average value of 0.215 °C (Fig. 5f). The H1975 cell temperature exceeded the environmental temperature for a duration of 590 s, representing 98.3 % of the entire process. While the maximum temperature of a single MCF7 cell was higher than that of an H1975 cell, the duration of the temperature exceeding 37 °C for the MCF7 cell was significantly shorter than that of the H1975 cell. Within the three types of tumor cells, the elevated temperature of the H1975 cell could be attributed to its more active metabolism. The temperature profile of a single H1975 cell resembled that of multiple H1975 cells [22]. The results indicated that this microfluidic chip, based on a sensor, can successfully capture a single tumor cell and precisely monitor slight temperature changes during regular metabolism on the chip.

To further investigate the potential application of this method, single MCF7 cell on chip was treated with 4 % paraformaldehyde and its temperature change was monitored for more than 1 h. As shown in Fig. 5g, within 30 min the fluctuation of cell's temperature was 0.064 °C between −0.026 and 0.167 °C, which was smaller than that of MCF7 cell under normal state. For approximately 95.5 % of the initial 30 min, the temperature of MCF7 cells exceeded the ambient temperature. As time progressed over the next 30 min, the average temperature fluctuation decreased to −0.012 °C (within the range of −0.1129 to 0.0666 °C). The duration of the temperature

exceeding 37 °C for the MCF7 cell decreased to 556 s, accounting for 30.9 % of the later 30 min. The temperature increment gradually approached 0, indicating a decline in cellular metabolic activity and ultimately leading to cell death. The single MCF7 cell on the chip was labeled red after calcein-AM/PI staining, indicating that the cell was dead (Fig. S5). In comparison to other single-cell thermometers like macro-size thermocouple probe [27,28] and temperature-sensitive material-based fluorometry [29], this microfluidic chip with a Pt sensor can trap single cell and provide an ideal environment for single cell growth. It enabled sensitive real-time monitoring of temperature changes with or without any stimulus and allowed for optical observation of cell states in-situ simultaneously. As a result, this microchip is capable of capturing single cell and monitoring its subtle temperature variations with high sensitivity, providing valuable insights into the physiological condition of individual cell.

4. Conclusion

In summary, an integrated microchip based on Pt thin-film electrodes was developed in this study for single-cell trapping, culture on-chip, and temperature monitor. A cell capture funnel-shaped well was designed to isolate a single cell from a cell suspension. High capture efficiency and good cell vitality were achieved for the MCF7 cells at the optimal flow rate. The Pt electrode-based thermometer in the integrated chip exhibited good linearity, high sensitivity, and low hysteresis error, thereby meeting the requirements for temperature detection at a single-cell level. With this integrated chip, single tumor cell (MCF7 cell, H1975 cell, and HepG2 cell) was trapped and cultured successfully. Our proposed system was utilized to determine the temperature increment of a single cell under normal physiological conditions or after exposure to a stimulus (4 % paraformaldehyde treatment). These results highlighted the potential of our system for applications in single-cellular analysis. However, the throughput of this sensor-based microfluidic chip is currently insufficient, making it difficult to monitor multiple individual cells within a single chip. The further study of our group will focus on improving the throughput of the Pt-based microfluidic chip for several individual cells at the same time. Furthermore, additional research is required to investigate the impact of cellular stress, the influence of the microenvironment on temperature measurements, and the correlation between temperature variations and specific physiological activities, such as epithelial-mesenchymal transition in tumor cells. Our microchip is currently being further optimized for long-term monitoring of a single cell and is a highly promising option for studying the relationship between the temperature variation and cellular event in single cell level.

Data availability statement

Data will be made available on request.

CRediT authorship contribution statement

Kai Chen: Project administration, Methodology, Writing – original draft. **Baihui Liang:** Funding acquisition, Project administration, Resources. **Ping Yang:** Methodology, Project administration. **Min Li:** Supervision, Methodology, Software. **Haojun Yuan:** Data curation, Formal analysis. **Jinlei Wu:** Software, Supervision. **Wanlei Gao:** Writing – review & editing, Project administration, Supervision. **Qinghui Jin:** Resources, Methodology, Investigation.

Declaration of competing interest

The authors declare that they have no known competing financial interests or personal relationships that could have appeared to influence the work reported in this paper.

Acknowledgments

This work was financially supported by the grant from the National Nature Science Foundation of China (No. 62201300, No. 82273681). This study was also supported by the special research funding from the Marine Biotechnology and Marine Engineering Discipline Group in Ningbo University and the Open Research Project of the State Key Laboratory of Industrial Control Technology, Zhejiang University, China (No. ICT2022B09).

Appendix A. Supplementary data

Supplementary data to this article can be found online at https://doi.org/10.1016/j.heliyon.2024.e30649.

References

[1] R. Shrestha, et al., A high-precision micropipette sensor for cellular-level real-time thermal characterization, Sensors 11 (9) (2011) 8826–8835.
[2] T. Yoo, et al., The real-time monitoring of drug reaction in HeLa cancer cell using temperature/impedance integrated biosensors, Sensor. Actuator. B Chem. 291 (2019) 17–24.
[3] T. Wu, et al., Intracellular thermal probing using aggregated fluorescent nanodiamonds, Adv. Sci. 9 (3) (2022) e2103354.

[4] M. Tellez-Gabriel, et al., Tumour heterogeneity: the Key advantages of single-cell analysis, Int. J. Mol. Sci. 17 (12) (2016).
[5] B. Deng, et al., Microfluidic cell trapping for single-cell analysis, Micromachines 10 (6) (2019).
[6] C. Feng, et al., Single-cell analysis of highly metastatic circulating tumor cells by combining a self-folding induced release reaction with a cell capture microchip, Anal. Chem. 93 (2) (2021) 1110–1119.
[7] G. Kucsko, et al., Nanometre-scale thermometry in a living cell, Nature 500 (7460) (2013) 54–58.
[8] Z. Han, et al., One-pot hydrothermal synthesis of nitrogen and sulfur co-doped carbon dots and their application for sensitive detection of curcumin and temperature, Microchem. J. 146 (2019) 300–308.
[9] S. Zhang, et al., Water-soluble luminescent gold nanoclusters reduced and protected by histidine for sensing of barbaloin and temperature, Microchem. J. 169 (2021).
[10] A. Kumar, et al., Synthesis and characterization of a fluorescent polymeric nano-thermometer: dynamic monitoring of 3D temperature distribution in co-cultured tumor spheroids, Analyst 148 (9) (2023) 2045–2057.
[11] T. Zhao, et al., Fluorescent polymeric nanoparticle for ratiometric temperature sensing allows real-time monitoring in influenza virus-infected cells, J. Colloid Interface Sci. 601 (2021) 825–832.
[12] Z. Gong, et al., Upconversion nanoparticle decorated spider silks as single-cell thermometers, Nano Lett. 21 (3) (2021) 1469–1476.
[13] L.Q. Huang, et al., Single-cell thermometry with a nanothermocouple probe, Chem. Commun. 59 (7) (2023) 876–879.
[14] F. Yu, et al., Highly luminescent gold nanocluster assemblies for bioimaging in living organisms, Chem. Commun. 58 (6) (2022) 811–814.
[15] K. Okabe, et al., Intracellular temperature mapping with a fluorescent polymeric thermometer and fluorescence lifetime imaging microscopy, Nat. Commun. 3 (2012) 705.
[16] F. Yang, et al., Measurement of local temperature increments induced by cultured HepG2 cells with micro-thermocouples in a thermally stabilized system, Sci. Rep. 7 (1) (2017) 1721.
[17] C.S.J. Li, Q. Wang, et al., Wireless thermometry for real-time temperature recording on thousand-cell level, IEEE Trans. Biomed. Eng. 66 (2019) 23–29.
[18] C. Li, et al., Real-time temperature measurements of HMEC-1 cells during inflammation production and repair detected by wireless thermometry, IEEE Trans. Biomed. Eng. 66 (7) (2018) 1898–1904.
[19] D. Rodoplu, et al., A micro-pupil device for point-of-care testing of viable Escherichia coli in tap water, Microchem. J. 178 (2022).
[20] W.-M. Liu, et al., Diversification of microfluidic chip for applications in cell-based bioanalysis, Chin. J. Anal. Chem. 40 (1) (2012) 24–31.
[21] Z.N. Wu, L. Lin, Nanofluidics for single-cell analysis, Chin. Chem. Lett. 33 (4) (2022) 1752–1756.
[22] X. Zhao, et al., A high-precision thermometry microfluidic chip for real-time monitoring of the physiological process of live tumour cells, Talanta 226 (2021) 122101.
[23] M.A. Fante, et al., Heat-inactivation of human serum destroys C1 inhibitor, pro-motes immune complex formation, and improves human T cell function, Int. J. Mol. Sci. 22 (5) (2021).
[24] J. Xu, et al., Temperature and growth selection effects on proliferation, differentiation, and adipogenic potential of Turkey myogenic satellite cells through frizzled-7-mediated wnt planar cell polarity pathway, Front. Physiol. 13 (2022) 892887.
[25] Y. Yamaguchi, et al., Development of a poly-dimethylsiloxane microfluidic device for single cell isolation and incubation, Sensor. Actuator. B Chem. 136 (2) (2009) 555–561.
[26] Y. Wang, et al., Single nanowire-based fluorescence lifetime thermometer for simultaneous measurement of intra- and extra-cellular temperatures, Chemical communications (Cambridge, England) (2023).
[27] C. Wang, et al., Determining intracellular temperature at single-cell level by a novel thermocouple method, Cell Res. 21 (10) (2011) 1517–1519.
[28] D.H. Han, et al., Non-interventional and high-precision temperature measurement biochips for long-term monitoring the temperature fluctuations of individual cells, Biosens. Bioelectron. 11 (11) (2021) 12.
[29] T.L. Wu, et al., Intracellular thermal probing using aggregated fluorescent nanodiamonds, Adv. Sci. 9 (3) (2022) 9.